

On the Barrier Properties of the Cornea: A Microscopy Study of the Penetration of Fluorescently Labeled Nanoparticles, Polymers, and Sodium Fluorescein

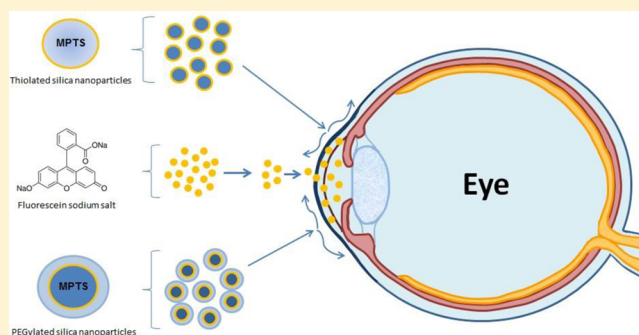
Ellina A. Mun, Peter W. J. Morrison, Adrian C. Williams, and Vitaliy V. Khutoryanskiy*

Reading School of Pharmacy, University of Reading, Whiteknights, Reading, RG6 6AD, United Kingdom

S Supporting Information

ABSTRACT: Overcoming the natural defensive barrier functions of the eye remains one of the greatest challenges of ocular drug delivery. Cornea is a chemical and mechanical barrier preventing the passage of any foreign bodies including drugs into the eye, but the factors limiting penetration of permeants and nanoparticulate drug delivery systems through the cornea are still not fully understood. In this study, we investigate these barrier properties of the cornea using thiolated and PEGylated (750 and 5000 Da) nanoparticles, sodium fluorescein, and two linear polymers (dextran and polyethylene glycol). Experiments used intact bovine cornea in addition to bovine cornea de-epithelialized or tissues pre-treated with cyclodextrin. It was shown that corneal epithelium is the major barrier for permeation; pretreatment of the cornea with β -cyclodextrin provides higher permeation of low molecular weight compounds, such as sodium fluorescein, but does not enhance penetration of nanoparticles and larger molecules. Studying penetration of thiolated and PEGylated (750 and 5000 Da) nanoparticles into the de-epithelialized ocular tissue revealed that interactions between corneal surface and thiol groups of nanoparticles were more significant determinants of penetration than particle size (for the sizes used here). PEGylation with polyethylene glycol of a higher molecular weight (5000 Da) allows penetration of nanoparticles into the stroma, which proceeds gradually, after an initial 1 h lag phase.

KEYWORDS: cornea, silica nanoparticles, PEGylated nanoparticles, permeation, β -cyclodextrin, fluorescence



INTRODUCTION

The eye is a complex organ with various tissues and cells, many of which are incapable of regeneration, including the corneal endothelium and the photoreceptor layer of the retina. Irreparable damage to these tissues, potentially resulting in blindness, can be caused by inflammation or ocular infection with microbial pathogens.¹ According to the World Health Organization, there are 285 million people living with serious vision disorders worldwide. Among them, 39 million people are blind. This number may rise to 76 million by 2020 without effective interventions. However, 75% of severe disorders including blindness can be treated and prevented.² Therefore, targeted drug delivery to the eye has become an area of significant research and interest for pharmaceutical scientists.

It is important for the eye to regulate the environment around ocular tissues. There are tight cellular barriers in the anterior and posterior parts of the eye that restrict the uptake of fluids and prevent penetration of foreign bodies. As a defensive function, ocular barriers also protect the eye from active pharmaceutical ingredients. The design of targeted ocular drug delivery systems to overcome these barriers remains one of the greatest challenges in pharmaceutical science.³ In treating major diseases of the posterior eye segment, such as age related

macular degeneration (the most common cause of blindness), retinal degeneration, diabetic retinopathy, and glaucoma, intravitreal drug administration is widely used.^{4–7} This invasive method is the most direct approach to deliver drugs to the posterior eye segment providing therapeutic tissue drug levels; however, it has serious potential side effects of retinal detachment, hemorrhage, endophthalmitis and cataract. Additionally, the repeated injections that are usually required are not well tolerated by patients.⁸ Therefore, this approach is considered to be potentially dangerous, and other less invasive methods are still needed.⁴

The most commonly used dosage form in treating ocular diseases is locally applied eye drops.^{3,9,5b} Topical administration of drugs is beneficial for delivery to the anterior (cornea, conjunctiva, sclera, anterior chamber) as well as posterior (vitreous humor, retina, choroid) segments of the eye. However, due to lachrymal drainage, systemic absorption, and biological barriers (principally the corneal epithelium), only a

Received: May 5, 2014

Revised: July 10, 2014

Accepted: August 22, 2014

Published: August 28, 2014

small fraction of the applied dose (less than 5%) reaches the intraocular tissues.^{3,10} In particular, it was reported to be extremely difficult to deliver drug to posterior segments of the eye, due to anatomy and physiology of the eye.^{5c} Following drug administration to the ocular surface, there are two main pathways by which the drug can enter the eye: either the corneal or conjunctival route.⁷ The latter is of minor relevance for the majority of drugs and is mostly the route of absorption for biopharmaceuticals (proteins or peptides) since the conjunctiva is permeable to hydrophilic and large molecules.³ However, most clinically used drugs are relatively small and lipophilic, hence, the corneal route usually dominates in ocular topical drug delivery.⁹

It is well-known that the cornea is a significant mechanical and chemical barrier to drug delivery. It is an optically transparent tissue that protects the inner parts of the eye.^{3,10} The diameter of the cornea is around 11.7 mm, and the thickness is 0.5–0.7 mm; the cornea is thicker in the center than in the limbus.¹⁰ The cornea consists of 5 layers: epithelium, Bowman's membrane, stroma, Descemet's membrane, and endothelium.¹¹ A cross section of bovine cornea with the epithelium, Bowman's membrane, and stroma highlighted can be seen in Figure S1 (Supporting Information).

Usually, the corneal epithelium is the main barrier restricting drug absorption into the eye.^{10,12} Stroma and endothelium, on the other hand, provide very little resistance to transcorneal permeation; as essentially aqueous layers, they inhibit permeation of only highly lipophilic compounds.^{13,14} The epithelium thickness is 50–90 μm , which is in a proportional relationship to stroma and endothelium as 1:10:0.1.¹⁰

In attempts to overcome the chemical and mechanical barriers, nanoparticles have been used to extend the residence time of formulations on the ocular mucosa and to increase corneal penetration of the drug. Nanoparticle-based drug delivery systems have shown promising results in ophthalmic research over the past 10 years.¹⁵ Positively charged nanoparticles, as drug carriers in iontophoresis studies, demonstrated higher penetration into anterior and posterior ocular structures compared to their negatively charged counterpart, ensuring prolonged therapeutic activity for more than 12 h post treatment.¹⁶ Nanoparticles with hydrolyzable dye were also shown to have high penetration rates overcoming both mechanical (epithelium tight junctions) and chemical (lipophilic epithelium and hydrophilic stroma) barriers of the cornea.¹⁷ Chitosan in the form of nanoparticles was more effective in interacting with ocular surfaces compared to solutions of linear polymer.¹⁸ Ammonium palmitoyl glycol chitosan-based nanoparticles facilitated the absorption of the anti-inflammatory drug prednisolone across the cornea, providing high levels of drug loading and significantly enhancing drug bioavailability.¹⁹ Another study using chitosan nanoparticles reported increased delivery of cyclosporin A to the corneal and conjunctival surfaces, providing long-term drug levels, but did not enhance the penetration of the drug into the inner part of the eye. The electrostatic interaction between positively charged chitosan and negatively charged cells of the cornea was suggested to be more responsible for the prolonged residence of cyclosporin A on the epithelial surface than mucoadhesive properties of chitosan.¹⁸ However, Calvo et al. demonstrated the opposite: the specific nature of chitosan was responsible for enhancing the ocular penetration of indomethacin rather than the positive surface charge of poly-*e*-

caprolactone (PECL) nanoparticles provided by chitosan and poly-L-lysine coatings.²⁰

Although there are a number of studies that have recently reported enhanced ocular drug delivery by using nanoparticles, the main factors limiting the passage of nanoparticulate drug carriers through the corneal barriers are still not fully understood: whether it is the size of nanoparticles or the presence of specific interactions between them and ocular surface. Therefore, in the current work, we studied the barrier functions of the cornea using two types of silica nanoparticles of different sizes with different surface chemistry: thiolated and PEGylated (750 and 5000 Da), fluorescently labeled with 5-(iodoacetamido)fluorescein (5-IAF) and contrasted with large and small (fluorescein–dextran and sodium fluorescein) molecular penetration. Permeation studies were conducted *in vitro*, using bovine corneas, on intact, pretreated with β -cyclodextrin, and scraped epithelium tissues.

■ EXPERIMENTAL SECTION

Materials. (3-Mercaptopropyl)trimethoxysilane (MPTS, 95%), methoxypolyethylene glycol maleimide with average molecular weights 750 and 5000 Da (PEG 750 and PEG 5000, respectively), 5-(iodoacetamido)fluorescein, sodium fluorescein (376 Da), fluorescein isothiocyanate dextran (4000 Da), *O*-[2-(3-mercaptopropionylamino)ethyl]-*O'*-methylpolyethylene glycol (5000 Da) (PEG 5000), 5,5'-dithiobis(2-nitrobenzoic acid) (DTNB), and L-cysteine hydrochloride were purchased from Sigma-Aldrich, Inc. (U.K.) and used as received. Dimethyl sulfoxide (DMSO) and sodium hydroxide (NaOH) were purchased from Fisher Scientific Ltd. (U.K.) and were laboratory grade reagents. OCT Embedding Matrix was also supplied by the same manufacturer. Additionally, β -cyclodextrin was purchased from TCI Europe N.V., Belgium, and used as received.

Synthesis of Thiolated Silica Nanoparticles. Thiolated silica nanoparticles were synthesized according to a protocol adapted from Mun et al.²³ Briefly, 0.75 or 0.38 mL of MPTS was mixed with 20 mL of DMSO and 0.5 mL of 0.5 mol/L NaOH aqueous solution (different volumes of MPTS resulted in the formation nanoparticles of groups A and B, respectively). The reaction was conducted under air bubbling and allowed to proceed for 24 h with permanent stirring at room temperature. Purification of nanoparticles was by dialysis against deionized water (5 L, 8 changes of water) with dialysis tubing of 12–14000 Da molecular weight cutoff (Medicell International Ltd, U.K.).

Ellman's Assay. Thiol-group content was determined by Ellman's assay.²¹ Briefly, 0.2–0.3 mg of freeze-dried nanoparticles was hydrated in 500 μL of phosphate buffer solution (0.5 mol/L, pH 8) and allowed to react with 500 μL of 5,5'-dithiobis(2-nitrobenzoic acid) (DTNB) (0.3 mg/mL) for 2 h. The absorbance was then measured at 420 nm (Epoch Microplate Spectrophotometer, BioTek Instruments, USA). The calibration curve was elaborated with cysteine hydrochloride solutions over the concentration range of 25–175 $\mu\text{mol/L}$.

Synthesis of Fluorescently Labeled Thiolated Silica Nanoparticles. Synthesized silica nanoparticles were labeled with 5-(iodoacetamido)fluorescein (5-IAF) similarly to the protocol described by Irmukhametova et al.²¹ Briefly, 3 and 0.3 mg of 5-IAF were added to 18 and 20 mL of aqueous dispersion of nanoparticles of 44 (group A) and 21 nm (group B), respectively. The amount of 5-IAF added was calculated

with regard to molar ratios such that 5 μmol of fluorophore was added to 50 μmol of SH groups of thiolated nanoparticles. The reaction mixture was stirred for 16 h at room temperature protected from light. Then, fluorescently labeled nanoparticles were purified by dialysis against deionized water in the dark according to the previously described protocol.²¹

PEGylation of Fluorescently Labeled Silica Nanoparticles. 5 mL of fluorescently labeled nanoparticles (5 mg/mL) was mixed with 100 mg of methoxypolyethylene glycol maleimide of two molecular weights (750 and 5000 Da). The reaction mixture was stirred during 16 h at room temperature protected from light. PEGylated nanoparticles were purified by dialysis in the dark as above.

Synthesis of Fluorescently Labeled PEG (5000 Da). 100 mg of methoxypolyethylene glycol maleimide 5000 Da was dissolved in 5 mL of deionized water, then 2 mg of 5-(iodoacetamido)fluorescein was added, and the reaction mixture was allowed to proceed for 16 h under permanent stirring at room temperature. Fluorescently labeled PEG 5000 (5-IAF-PEG) was purified by dialysis against deionized water (5 L, 8 changes of water in total) using cellulose membranes with 100–500 Da molecular weight cutoff (Spectrum Laboratories Inc., CA, USA).

Preparation of Solutions. 0.5 and 2 mg of sodium fluorescein (376 Da) and fluorescein isothiocyanate dextran (FITC-dextran, 4000 Da), respectively, were each dissolved in 10 mL of deionized water and were left for 5 h under permanent stirring at room temperature. 30 mL of β -cyclodextrin solution was prepared at 20 mg/mL by dissolving in deionized water at 60 °C under permanent stirring followed by cooling of the solution to physiological temperature before use.

The “Whole Eye” Method for Studying the Permeability of Silica Nanoparticles. Permeation studies were conducted using the “whole eye” method to avoid the risk of corneal swelling observed when employing Franz diffusion cells with fully dissected tissues.²⁹ Bovine eyes used in these experiments were obtained from P.C. Turner Abattoir (Hampshire, U.K.). Freshly extracted eyes, with the cornea covered by the lid, were transported to the laboratory in a cold box and stored in the fridge at 4 °C overnight prior to use, shown in our earlier work to have no adverse effects on tissue barrier properties.²⁹ For permeation studies, each eye was placed into a glass beaker with the Franz cell donor compartment on top, secured with a cling film (Figure S2, Supporting Information). The central cornea of the eye was then exposed to 1 mL of one of the solutions: thiolated, PEGylated (750 Da), or PEGylated (5000 Da) nanoparticle dispersion (5 mg/mL) for 2 h. For experiments with pretreated and removed corneal epithelium, some pretreatment procedures were carried out prior to nanoparticle exposure. In the former case, the eye was exposed to 1 mL of β -cyclodextrin aqueous solution (20 mg/mL) for 1 h, after which this solution was withdrawn with a syringe. In the latter case, the epithelium layer was carefully scraped off the cornea with a metal spatula. These procedures were followed by exposing the eye to one of the nanoparticle solutions.

All experiments were conducted in triplicate, in a water bath at 37 °C. After 2 h treatment, the cornea was extracted from the eye, and the area exposed to the sample solutions was excised using a sharp blade. Three different segments of each cornea were mounted in OCT and kept on dry ice. Cross sectioning (7 μm thick sections) of each corneal segment was performed on a

cryostat (Bright, model OTF)/microtome (Bright, model 5040) and fixed in groups of six on 75 mm \times 25 mm glass slides followed by application of 50–75 μL of 4',6-diamidino-2-phenylindole (DAPI; 1.5 $\mu\text{g}/\text{mL}$) to stain the cell nuclei.

Fluorescence Microscopy. Cross sections of cornea were examined using fluorescence microscopy (Zeiss Imager A1 with AxioCam MRm Zeiss camera); each image was taken using DAPI (blue, maximum $\lambda_{\text{emission}} = 461 \text{ nm}$) and Fluor (green, maximum $\lambda_{\text{emission}} = 519 \text{ nm}$) filters and then overlaid as a composite image.

Dynamic Light Scattering. The size of fluorescently labeled silica nanoparticles was determined using dynamic light scattering with a Nano-ZS series (Malvern Instruments, U.K.) at 25 °C. Each sample was analyzed three times, and the average hydrodynamic diameters are presented as a mean value \pm standard deviation.

Fluorescence Spectroscopy. Fluorescence spectra were recorded for fluorescently labeled thiolated and PEGylated nanoparticles using a FP-6200 spectrofluorometer (Jasco, U.K.) over the wavelength range 505–700 nm ($\lambda_{\text{ex}} = 492 \text{ nm}$).

RESULTS AND DISCUSSION

Synthesis and Characterization of Silica Nanoparticles. Synthesis of thiolated silica nanoparticles in DMSO was previously reported by Irmukhametova et al.^{21,22} resulting in $55 \pm 4 \text{ nm}$ particles. Recently, we also reported a slightly modified synthetic protocol,²³ which was used in the present study. The reaction mixture containing 0.2 mol/L MPTS was bubbled with atmospheric air providing additional cross-linking via S–S bridges and resulting in the formation of nanoparticles of $45 \pm 1 \text{ nm}$ (subsequently referred to as group A). The concentration of MPTS in the reaction mixture is one factor controlling the size of nanoparticles; halving the concentration of MPTS for the synthesis (0.1 mol/L) formed smaller nanoparticles, $21 \pm 1 \text{ nm}$ (subsequently referred to as group B).

Silica nanoparticles were fluorescently labeled with 5-(iodoacetamido)fluorescein (5-IAFL) by reaction with 5-IAFL (Figure S3, Supporting Information). The fluorophore was added into the reaction mixture in a ratio of 5:50 μmol with regard to the number of SH groups of silica nanoparticles; thus there remained thiol groups available for further PEGylation of some of the fluorescently labeled samples.

Samples of fluorescently labeled thiolated silica nanoparticles of each size (44 and 21 nm) were PEGylated with methoxypolyethylene glycol maleimide of two molecular weights (750 and 5000 Da). Two groups of nanoparticles were produced:

1. A: consisting of 44 nm thiolated and PEGylated (750 and 5000 Da) nanoparticles
2. B: consisting of 21 nm thiolated and PEGylated (750 and 5000 Da) nanoparticles

The DLS distributions demonstrate the greater sizes of PEGylated nanoparticles due to the presence of a PEG corona on their surfaces (Figure 1 and Table 1). Comparison of the sizes of thiolated and PEGylated nanoparticles was conducted using Anova software (Tukey's multiple comparison test) revealing significant differences between each sample within the groups A ($p < 0.001$) and B ($p < 0.05$ and $p < 0.001$). The increase in size was 9 and 24 nm in group A and 6 and 22 nm in group B for PEG750 and PEG5000 nanoparticles, respectively, compared to thiolated particles.

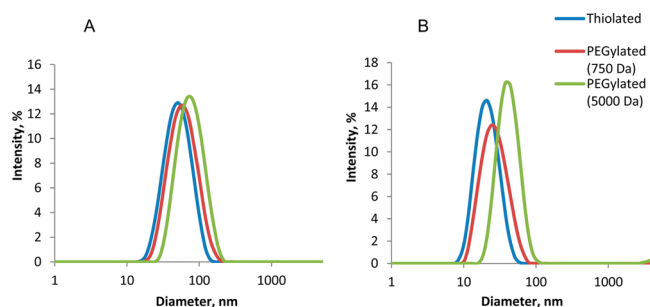


Figure 1. Size distribution of thiolated and PEGylated nanoparticles of groups A and B, fluorescently labeled with 5-IAFL.

Due to the screening effect of PEG shells, reduced 5-IAFL fluorescence intensities were observed for PEGylated nanoparticles. PEG of a larger molecular weight provided the lowest intensity since screening with PEG5000 Da is greater than with PEG750 Da (Figure S4, Supporting Information). These results are in good agreement with our previously reported observations for PEGylation of silica nanoparticles labeled with Alexa Fluor maleimide.²³

The general characteristics of fluorescently labeled silica nanoparticles are summarized in Table 1.

As seen from this table, the polydispersity index (PDI) values for both groups A and B decrease on PEGylation. This can be explained by the formation of PEG-based polymer shells around the silica cores that prevent the nanoparticles from aggregating via disulfide bridges. The parent thiolated silica nanoparticles do show some tendency to aggregate due to disulfide bridge formation, which results in higher PDI values.

Comparative Permeability Studies on Intact and Pretreated with β -Cyclodextrin Corneal Epithelium.

Franz diffusion cells have been widely employed for *in vitro* transcorneal permeation studies for many years.^{24–28} However, corneal swelling was observed when using Franz cells, and dissected ocular tissues undergo structural changes with time. To overcome these drawbacks, the “whole eye” method was developed.²⁹

Sodium fluorescein salt was initially used as a model agent, since corneal permeation of this low molecular weight compound was previously reported.^{30,31} After 2 h of exposure of bovine eye to sodium fluorescein, fluorescence micrographs show penetration of this dye through the epithelium into the stroma. However, this fluorescent probe is not evenly distributed throughout all parts of the cornea: in some areas sodium fluorescein is observed in the stroma within 2 h of dosing whereas other areas show no permeation through the epithelium after 2 h exposure (shown in Figure 2).

Although the corneal epithelium is permeable to low molecular weight compounds, its tight junctions restrict the passage of larger molecules. The maximum molecular weight that can permeate through the cornea was reported to be 500

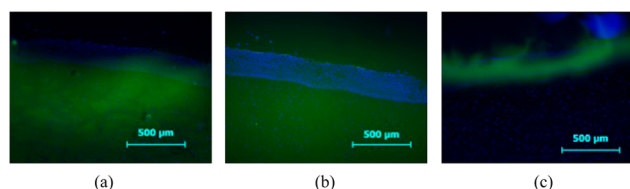


Figure 2. Exemplar fluorescence micrographs of cross section of bovine cornea (corneal epithelium is shown in blue) with sodium fluorescein (green). Scale bar: 500 μm . Images a, b, and c were taken from different regions of the same eye.

Da,³² but an earlier study by Huang et al.¹⁴ showed that the cornea is only impermeable to molecules larger than 5000 Da. Our experiments indicate that sodium fluorescein, a water-soluble compound with a molecular weight of 376 Da, penetrates into and permeates through the corneal epithelial membrane. Thus, to explore the molecular weight selectivity of this membrane, larger compounds, namely, FITC-dextran (4000 Da) and 5-IAF-PEG (5000 Da), were used to study molecular weight effects on corneal permeation. FITC-dextran was selected as a material close to the molecular weight of PEG (5000 Da) that we used in functionalizing silica nanoparticles. As higher molecular weight compounds, neither FITC-dextran nor 5-IAF-PEG 5000 permeated through the corneal epithelium, but instead formed a layer on its surface which is seen as a green band in Figure 3.

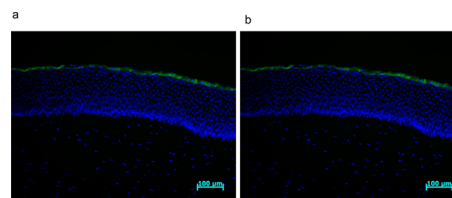


Figure 3. Exemplar fluorescence micrographs of cross section of bovine cornea (blue) with FITC-dextran 4000 Da (a) and 5-IAF-PEG 5000 Da (b) (green). Each experiment was performed in triplicate using different eyes. Size bar: 100 μm .

Cyclodextrins are well-known to enhance penetration into biological barriers, such as skin and cornea, and so improve the bioavailability of topically applied drugs.^{33,34} They are water-soluble cyclic oligosaccharides with a lipophilic central cavity and a hydrophilic outer surface, containing six, seven, or eight glucopyranose units. Aqueous cyclodextrin solutions were shown to disrupt the corneal epithelium integrity by extracting cholesterol and other lipids from ocular membranes, making the corneal barrier less resistant to permeation of hydrophilic and hydrophobic compounds.²⁹ Additionally, the same study reported β -cyclodextrin to be the most effective (among other

Table 1. Characteristics of Thiolated and PEGylated Nanoparticles of Groups A and B, Fluorescently Labeled with 5-IAFL

group	sample name	diameter, nm	PDI	nanoparticle concn, mg/mL	max emission, nm	max intensity
A	thiolated	45 \pm 1	0.332	5	515	505
	PEGylated (750 Da)	54 \pm 1	0.194	5	517	443
	PEGylated (5000 Da)	69 \pm 2	0.145	7	516	415
B	thiolated	21 \pm 1	0.263	4	515	336
	PEGylated (750 Da)	27 \pm 1	0.254	4	515	146
	PEGylated (5000 Da)	43 \pm 3	0.231	6	515	132

types of cyclodextrins) in enhancing permeability of riboflavin through fresh and cryopreserved corneas.²⁹

Applying β -cyclodextrin solution onto the bovine eye for 1 h, before removal and the dosing with fluorescent marker solutions, enhanced the penetration of sodium salt fluorescein. The stroma images were analyzed with ImageJ software for the cornea treated with β -cyclodextrin and an untreated one. Compared to dye distribution for nontreated cornea, β -cyclodextrin pretreatment produced more homogeneous distribution of sodium fluorescein in the stroma, observed across the whole exposed area of the cornea (Figure 4).

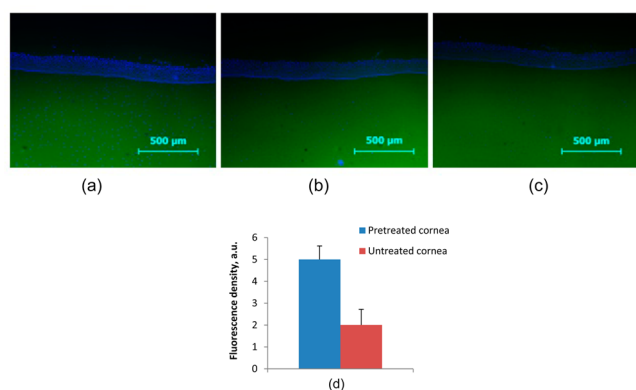


Figure 4. Penetration of sodium fluorescein into the bovine cornea pretreated with β -cyclodextrin. Images a, b, c were taken from experiments with the same eye. Scale bar: 500 μm ; fluorescence density (fluorescence intensity/area) of sodium fluorescein in the stroma pretreated with β -cyclodextrin and untreated cornea, analyzed with ImageJ software (10 images were analyzed of each sample) (d).

Although there are studies reporting the delivery of dextrans up to 4 and 70 kDa into the cornea, enhanced with borneol and anodal iontophoresis,^{30,35} applying β -cyclodextrin prior to exposing the cornea to either FITC-dextran 4000 Da or PEG 5000 did not demonstrate any permeation enhancement of these compounds (Figure 5). There is evident disruption of the

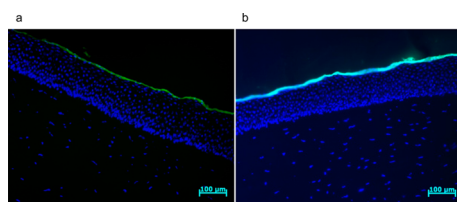


Figure 5. Exemplar fluorescence micrographs of cross section of bovine cornea, pretreated with β -cyclodextrin, exposed to FITC-dextran 4000 Da (a) and 5-IAFL-PEG 5000 Da (b). Each experiment was performed in triplicate using different eyes. Size bar: 100 μm .

epithelium layer caused by the treatment with β -cyclodextrin in agreement with our previous report;²⁹ however, FITC-dextran 4000 Da and PEG 5000 Da were only observed on the corneal surface, suggesting that the integrity of the cornea was not disrupted sufficiently for the larger molecules to penetrate.

Nanomaterials have been employed in various in vitro corneal permeation experiments, including the use of carboxymethyl tamarind kernel polysaccharide nanoparticles,³⁶ thiolated pectin nanoparticles,³⁷ and droplet nanosized α -tocopherol emulsion formulations.^{38a} These studies reported enhanced permeation of tropicamide, timolol maleate, and

indometacin from the nanosystems using dissected cornea. The “whole eye” method provides experimental in vitro conditions that are closer to the in vivo situation because this model avoids potential artifacts when using removed ocular tissue in Franz diffusion cells. However, it should be borne in mind that periocular and choroid clearance mechanisms are absent when in vitro models are used.^{38b} To investigate the permeability of bovine cornea to nanoparticle-type formulations, three types of silica nanoparticles of group A (thiolated and PEGylated with PEG of two molecular weights, 750 and 5000 Da), were applied onto the bovine eye. Fluorescence microscopy images suggest that none of these nanoparticles penetrated the cornea, even for the epithelium treated with β -cyclodextrin (Figure 6).

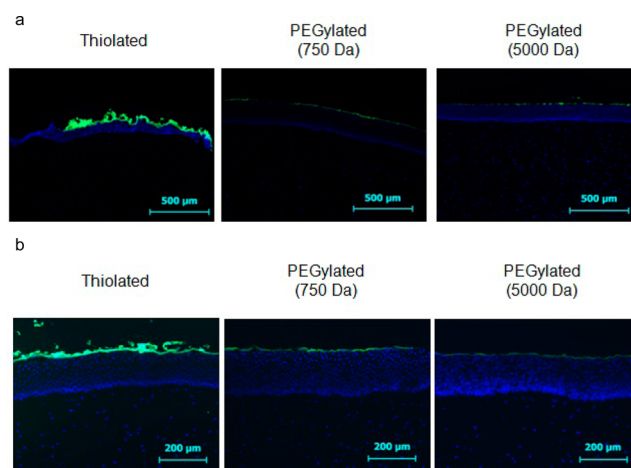


Figure 6. Exemplar fluorescence micrographs of cross section of bovine cornea with intact (a) and pretreated with β -cyclodextrin (b) epithelium, exposed to silica nanoparticles of group A ranging from 45 to 69 nm diameters. Size bar: 500 μm (a), 200 μm (b). Each experiment was performed in triplicate with different eyes.

The ocular surface is one of the mucosal tissues in the human body that are coated by a mucus layer of glycoproteins (mucins) with cysteine-containing domains.³⁹ The mucus layer, secreted by conjunctival goblet cells, is part of a three layered structure of the precorneal tear film. This film plays an important role in forming a continuous fluid layer over the cornea, keeping it moist, protecting it from bacterial infections, providing lubrication for the movement of the eyelids, and removing foreign bodies from its surface. According to the “three layers theory” of the precorneal tear film, the mucus layer was believed to be the innermost one, beneath the superficial oily and middle aqueous layers.¹¹ However, others report that the mucus is present throughout the tear film.⁴⁰

Bernkop-Schnurch et al.⁴¹ reported that thiolated (thiol bearing side chains) polymers are able to covalently bond to mucins via disulfide bridges, which markedly improves their mucoadhesive properties. In addition, poly(vinylpyrrolidone)/poly(acrylic acid)-cysteine thiomers nanoparticles were demonstrated to enhance the delivery of insulin by prolonging its residence time on the stomach mucosa due to the covalent bond formation between cysteine domains of mucin and PAA.⁴² Similarly to thiomers, thiolated silica nanoparticles were reported to have excellent mucoadhesive properties assessed by evaluating their retention time on bovine ocular surfaces.²¹ However, their PEGylated counterpart demonstrated significantly lower mucoadhesion. In agreement with Irmukhametova et al.,²¹ our thiolated silica nanoparticles (SH-group content =

$249 \pm 30 \mu\text{mol/g}$) were observed on the corneal surface indicating no permeation, due to disulfide bond formation between the thiol groups of nanoparticles and cysteine groups of mucins. These interactions may be a limiting factor in penetration of thiolated nanoparticles into bovine cornea. Upon PEGylation, a number of SH groups of thiolated nanoparticles is screened by PEG, and this effect is more significant with larger PEG. For example, the SH-group content for nanoparticles PEGylated with 750 Da PEG was $95 \pm 6 \mu\text{mol/g}$, whereas for 5000 Da PEG it was $78 \pm 5 \mu\text{mol/g}$. Therefore, the interactions between nanoparticles and the mucus layer of the cornea are considerably reduced by PEGylation. However, neither PEGylated 750 nor 5000 Da nanoparticles can penetrate into the cornea, which suggests that the nanoparticle size (greater for PEGylated nanoparticles, Table 1) is a further factor limiting penetration.

To test the barrier function of bovine cornea to smaller nanoparticles, thiolated and PEGylated nanoparticles of group B were applied onto the eye surface with intact and pretreated with β -cyclodextrin epithelium. Again, no penetration for any of these smaller nanoparticles was observed, which suggests that the tight junctions of the corneal epithelium prevent penetration of any particles into the eye surface, even as small as $21 \pm 1 \text{ nm}$ (Figure S5, Supporting Information). For thiolated nanoparticles, the presence of SH groups forms an additional barrier due to the attractive mucoadhesive interactions with mucosal surface of the eye. Applying β -cyclodextrin improved penetration of sodium fluorescein by partially disrupting epithelium tight junctions, but this disruption of corneal integrity is not sufficient to allow nanoparticle penetration.

Ocular Permeability Studies of Silica Nanoparticles with Removed Epithelium. Stroma is known to be more permeable to larger molecules than epithelium.¹¹ To investigate if stroma also acts as a barrier to nanoparticle penetration, silica nanoparticles of groups A and B were applied onto the bovine eye, following the same experimental protocol, but with the epithelium layer removed prior to nanoparticle exposure. The epithelium layer is removed as a gel, and the visual difference between the intact bovine eye and the one with removed epithelium confirmed removal of this layer (Figure S6, Supporting Information).

The physical removal of epithelium is currently used as an initial stage of a procedure to treat some ocular conditions such as keratoconus. This de-epithelialization allows enhanced permeability of riboflavin, which is used in corneal cross-linking.⁴³ Stroma has a relatively open “gel-like” structure allowing the diffusion of compounds with a molecular weight below 500 000 Da.¹¹ Corneal stroma mainly consists of regularly arranged collagen fibers and keratocytes, which are responsible for repair and maintenance. Before 1982, it was believed that the only collagen type present in corneal stroma is type I, however it was demonstrated for the first time by Newsome and co-workers⁴⁴ and later confirmed by another group^{45,46} that corneal stroma consists of different types of collagen including type III, which contains cysteine and cysteine domains. In addition, Saika et al.⁴⁷ reported that collagen type III is produced in higher proportions than collagen type I in the early stages of the healing process.

The interactions between cysteine domains of the corneal stroma and sulfhydryl groups of thiolated silica nanoparticles are believed to be a limiting barrier in nanoparticle permeation rather than their size. To test this hypothesis, thiolated and

PEGylated silica nanoparticles of groups A and B were applied onto the bovine eyes with removed epithelium according to the above-described protocol (Figure 7).

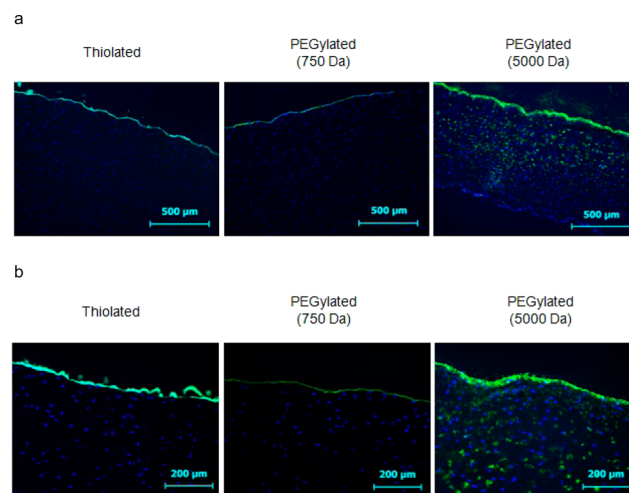


Figure 7. Exemplar fluorescence micrographs of cross sections of de-epithelialized bovine cornea, exposed to silica nanoparticles of groups A (a) and B (b) for 2 h. Each experiment was performed in triplicate using different eyes. Size bar: 500 μm (a), 200 μm (b).

It is seen that thiolated nanoparticles, due to the interactions of SH groups with cysteine domains of the stroma, do not penetrate into the eye, even with the epithelial layer removed, and this is not affected by nanoparticle size (Figure 7a,b). These particles tend to adhere to the stromal surface, which is in agreement with an earlier study reporting the mucoadhesive properties of thiolated silica nanoparticles.²¹ Upon PEGylation with PEG maleimide of 750 Da, some thiol groups are screened by the polymer, but a significant number of SH groups ($[\text{SH}] = 95 \pm 6 \mu\text{mol/g}$) remain available for binding to cysteine-rich domains of the stroma. Therefore, there is still no penetration observed for PEGylated (750 Da) nanoparticles. However, when PEG maleimide of a higher molecular weight (5000 Da) was used, nanoparticles of both types (groups A and B, $69 \pm 2 \text{ nm}$ and $43 \pm 3 \text{ nm}$, respectively) penetrated into the ocular stroma. This is likely to be due to the larger number of thiol groups substituted with PEG of a greater molecular weight ($[\text{SH}] = 78 \pm 5 \mu\text{mol/g}$), compared to PEG 750, and also the large and bulky PEG chains surrounding the remaining surface SH groups, effectively screening the thiol groups and preventing them from interacting with cysteine domains of the ocular stroma. The enhanced permeation of PEGylated nanoparticles is in agreement with the findings reported by Hanes et al., who have reported that PEGylated nanoparticles do not interact with biological tissues, such as human mucus, due to strong hydrophilicity and neutral charge provided by PEG coating, which helps the diffusion of nanoparticles.^{48,49} PEGylation was also demonstrated to improve cytoplasmic transport of nanoparticles⁵⁰ and penetration into vitreous gel studied using fresh bovine vitreous.⁵¹

Our materials were designed to enable particle size effects and surface chemistry effects to be interrogated as determinants of nanoparticle penetration and permeation. Thus, two different nanoparticles (thiolated of group A and PEGylated 5000 Da nanoparticles of group B) are a similar size ($45 \pm 1 \text{ nm}$ and $43 \pm 3 \text{ nm}$, respectively; *t* test, $p = 0.335$), but with different surface coverage ($[\text{SH}] = 249 \pm 30$ and $41 \pm 3 \mu\text{mol/g}$,

respectively). While the sizes are consistent, the differences in surface chemistries and consequent mucoadhesion provide different levels of penetration, illustrating that the interactions between the ocular surface and nanoparticles is the limiting factor for ocular penetration and not the particle size of these particular materials when the epithelium is removed.

To explore the time course of nanoparticle uptake, the bovine eyes with removed epithelium were exposed to thiolated and PEGylated nanoparticles of group A for 0.5 and 1 h (Figure 8).

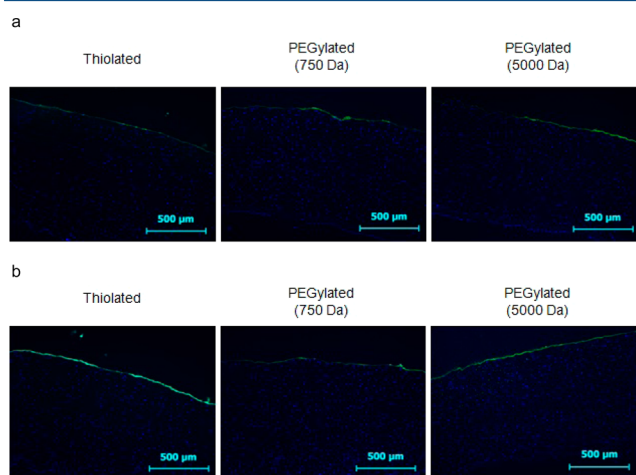


Figure 8. Exemplar fluorescence micrographs of cross section of bovine cornea with removed epithelium, exposed to silica nanoparticles of group A for 0.5 h (a) and 1 h (b). Each experiment was performed in triplicate using different eyes. Size bar: 500 μm .

No difference in penetration of thiolated and PEGylated 750 Da nanoparticles (group A) upon 0.5 and 1 h of exposure time was observed, compared to 2 h, confirming no penetration of those nanoparticles through the ocular stroma for the reasons described above. However, the distribution of PEGylated 5000 Da nanoparticles varies with exposure time: there was no penetration observed after 0.5 h exposure, whereas some nanoparticles are clearly present in the stroma after 1 h, but not to the extent of penetration after 2 h of exposure. To evaluate the degree of penetration of PEGylated 5000 Da nanoparticles at different times, the fluorescence micrographs were analyzed and the fluorescence intensity in the stroma was assessed using ImageJ software (Figure 9).

CONCLUSIONS

In the present work, the barrier functions of the cornea were studied using small and large molecular weight fluorescent probes and thiolated and PEGylated (750 and 5000 Da) nanoparticles. The “whole eye” method was employed to avoid corneal swelling and structural changes it might undergo when using isolated cornea in Franz diffusion cells. In agreement with previous publications, it was shown that the epithelium is the major limiting barrier to penetration and permeation. β -Cyclodextrin disrupts integrity of the epithelium providing higher permeation of low molecular weight compounds, such as sodium fluorescein, but not enhancing the permeability of larger molecules and nanoparticles. To investigate the limiting factors for nanoparticle permeation (size or possible interactions with corneal surface), further experiments were conducted with removed epithelium. Nanoparticles of two

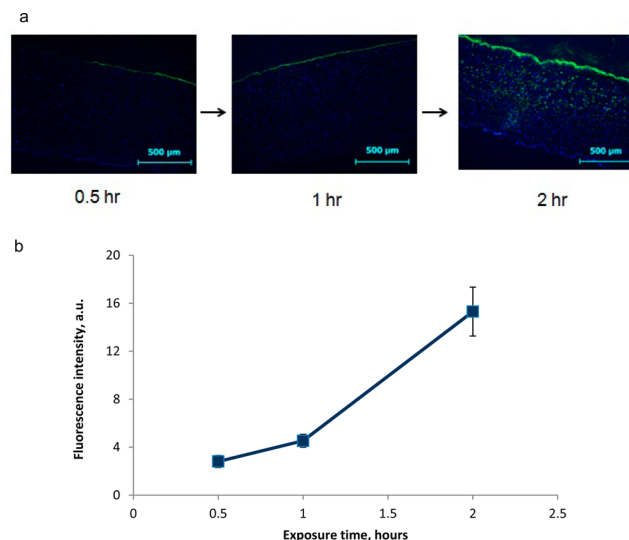


Figure 9. Exemplar fluorescence micrographs of PEGylated (5000 Da) nanoparticles in the stroma (a). Fluorescence intensity of PEGylated (5000 Da) nanoparticles in the stroma at different exposure times, analyzed with ImageJ software (6 images of each sample were analyzed, and mean \pm SD are presented) (b).

groups were applied. Comparison of two types of nanoparticles of the same size and different number of SH groups on the surface revealed that the binding of nanoparticles to collagen is a more important factor that prevents their penetration through the de-epithelialized ocular tissues, and this phenomenon does not depend on the particle size. PEGylation with PEG of a higher molecular weight (5000 Da) provides screening of the majority of thiol groups on the surface of nanoparticles, allowing the passage of PEGylated nanoparticles into the stroma. However, thiolated and PEGylated (750 Da) nanoparticles, possessing adhesive properties, stay on the ocular surface. The permeation of PEGylated (5000 Da) nanoparticles into the stroma proceeds gradually, starting after 1 h, reaching over 15 au of fluorescence intensity in the stroma at 2 h of the exposure time.

ASSOCIATED CONTENT

Supporting Information

A cross section of the bovine cornea with main layers highlighted; a scheme of the “whole eye” method; schematic representation of fluorescein-labeling reaction of thiolated silica nanoparticles; fluorescence spectra of thiolated and PEGylated nanoparticles; exemplar fluorescence micrographs of cross section of bovine cornea with intact and pretreated with β -cyclodextrin epithelium, exposed to silica nanoparticles of group B; images of epithelium layer removal. This material is available free of charge via the Internet at <http://pubs.acs.org>.

AUTHOR INFORMATION

Corresponding Author

*E-mail: v.khutornyanskiy@reading.ac.uk. Reading School of Pharmacy, University of Reading, Whiteknights, PO Box 224, Reading RG6 6AD, United Kingdom.

Notes

The authors declare no competing financial interest.

ACKNOWLEDGMENTS

E.A.M. is grateful to University of Reading for International Postgraduate Research Studentship. P.W.J.M. acknowledges BBSRC for Doctoral Training Grant (BB/F017189/1). The authors are grateful to P.C. Turner Abattoir (Hampshire, U.K.) for providing bovine eyes for experiments.

REFERENCES

- (1) Yorio, T.; Clark, A. F.; Wax, M. B. Ocular Therapeutics; *Eye on New Discoveries*; Elsevier: 2008; pp 3–30.
- (2) World Health Organization [http://www.who.int/blindness/history/en/].
- (3) Hornof, M.; Toropainen, E.; Uttri, A. Cell culture models of the ocular barriers. *Eur. J. Pharm. Biopharm.* **2005**, *60*, 207–225.
- (4) Ranta, V. P.; Urtti, A. Transscleral drug delivery to the posterior eye: Prospects of pharmacokinetic modeling. *Adv. Drug Delivery Rev.* **2006**, *58*, 1164–1181.
- (5) (a) Laude, A.; Tan, L. E.; Wilson, C. G.; Lascaratos, G.; Elashry, M.; Aslam, T.; Patton, N.; Dhillon, B. Intravitreal therapy for neovascular age-related macular degeneration and inter-individual variations in vitreous pharmacokinetics. *Prog. Retinal Eye Res.* **2010**, *29*, 466–475. (b) Wilson, C. G. Topical drug delivery in the eye. *Exp. Eye Res.* **2004**, *78*, 737–743. (c) Hughes, P. M.; Olejnik, O.; Chang-Lin, J.-E.; Wilson, C. G. Topical and systemic drug delivery to the posterior segments. *Adv. Drug Delivery Rev.* **2005**, *57*, 2010–2032.
- (6) Bochot, A.; Fattal, E. Liposomes for intravitreal drug delivery: A state of the art. *J. Controlled Release* **2012**, *161*, 628–634.
- (7) Thrimawithana, T. R.; Young, S.; Bunt, C. R.; Green, C.; Alany, R. G. Drug delivery to the posterior segment of the eye. *Drug Discovery Today* **2011**, *16*, 270–277.
- (8) Geroski, D. H.; Edlhauser, H. F. Drug delivery for posterior segment eye disease. *Invest. Ophthalmol. Visual Sci.* **2000**, *41*, 961–964.
- (9) Urtti, A. Challenges and obstacles of ocular pharmacokinetics and drug delivery. *Adv. Drug Delivery Rev.* **2006**, *58*, 1131–1135.
- (10) Jarvinen, K.; Jarvinen, T.; Urtti, A. Ocular absorption following topical delivery. *Adv. Drug Delivery Rev.* **1995**, *16*, 3–19.
- (11) Washington, N.; Washington, C. and Wilson, C. G. Physiological Pharmaceutics. Barriers to drug absorption, 2nd ed.; Taylor and Francis: 2001; pp 249–270.
- (12) Hillery, A. M.; Lloyd, A. W.; Swarbrick, J. Drug delivery and targeting for pharmacists and pharmaceutical scientists; CRC Press: 2001; pp 329–353.
- (13) Huang, H. S.; Schoenwald, R. D.; Lach, J. L. Corneal penetration behavior of beta-blocking agents II: assessment of barrier contributions. *J. Pharm. Sci.* **1983**, *72*, 1272–1279.
- (14) Huang, A. J. W.; Tseng, S. C. G.; Kenyont, K. R. Paracellular permeability of corneal and conjunctival epithelia. *Invest. Ophthalmol. Visual Sci.* **1989**, *30*, 684–689.
- (15) Sahoo, S. K.; Dilnawaz, F.; Krishnakumar, S. Nanotechnology in ocular drug delivery. *Drug Discovery Today* **2008**, *13*, 144–151.
- (16) Eljarrat-Binstock, E.; Orucov, F.; Aldouby, Y.; Frucht-Pery, J.; Domb, A. J. Charged nanoparticles delivery to the eye using hydrogel iontophoresis. *J. Controlled Release* **2008**, *126*, 156–161.
- (17) Baba, K.; Tanaka, Y.; Kubota, A.; Kasai, H.; Yokokura, S.; Nakanishi, H.; Nishida, K. A method for enhancing the ocular penetration of eye drops using nanoparticles of hydrolyzable dye. *J. Controlled Release* **2011**, *153*, 278–287.
- (18) Campos, A. M.; Sanchez, A.; Alonso, M. J. Chitosan nanoparticles: a new vehicle for the improvement of the delivery of drugs to the ocular surface. Application to cyclosporine A. *Int. J. Pharm.* **2001**, *224*, 159–168.
- (19) Qu, X.; Khutoryanskiy, V. V.; Stewart, A.; Rahman, S.; Papahadjopoulos-Sternberg, B.; Dufes, C.; McCarthy, D.; Wilson, C. G.; Lyons, R.; Carter, K. C.; Schatzlein, A.; Uchegbu, I. F. Carbohydrate-based micelle clusters which enhance hydrophobic drug bioavailability by up to 1 order of magnitude. *Biomacromolecules* **2006**, *7*, 3452–3459.
- (20) Calvo, P.; Vila-Jato, J. L.; Alonso, M. J. Evaluation of cationic polymer-coated nanocapsules as ocular drug carriers. *Int. J. Pharm.* **1997**, *153*, 41–50.
- (21) Irmukhametova, G. S.; Mun, G. A.; Khutoryanskiy, V. V. Thiolated mucoadhesive and PEGylated non-mucoadhesive organosilica nanoparticles from 3-mercaptopropyltrimethoxysilane. *Langmuir* **2011**, *27*, 9551–9556.
- (22) Irmukhametova, G. S.; Fraser, B. J.; Keddie, J. L.; Mun, G. A.; Khutoryanskiy, V. V. Hydrogen-Bonding-Driven Self-Assembly of PEGylated Organosilica Nanoparticles with Poly(acrylic acid) in Aqueous Solutions and in Layer-by-Layer Deposition at Solid Surfaces. *Langmuir* **2012**, *28*, 299–306.
- (23) Mun, E. A.; Hannell, C.; Rogers, S. E.; Hole, P.; Williams, A. C.; Khutoryanskiy, V. V. On the Role of Specific Interactions in the Diffusion of Nanoparticles in Aqueous Polymer Solutions. *Langmuir* **2014**, *30*, 308–317.
- (24) Suhonen, P.; Jarvinen, T.; Koivisto, S.; Urtti, A. Different effects of pH on the permeation of pilocarpine and pilocarpine prodrugs across the isolated rabbit cornea. *Eur. J. Pharm. Sci.* **1998**, *6*, 169–176.
- (25) Tegtmeier, S.; Papanitiou, I.; Muller-Goymann, C. C. Reconstruction of an in vitro cornea and its use for drug permeation studies from different formulations containing pilocarpine hydrochloride. *Eur. J. Pharm. Biopharm.* **2001**, *51*, 119–125.
- (26) Baydoun, L.; Muller-Goymann, C. C. Influence of n-octenylsuccinate starch on in vitro permeation of sodium diclofenac across excised porcine cornea in comparison to Voltaren ophtha. *Eur. J. Pharm. Biopharm.* **2003**, *56*, 73–79.
- (27) Reichl, S.; Dohring, S.; Bednarz, J.; Muller-Goymann, C. C. Human cornea construct HCC—an alternative for in vitro permeation studies? A comparison with human donor corneas. *Eur. J. Pharm. Biopharm.* **2005**, *60*, 305–308.
- (28) Friedrich, I.; Reichl, S.; Muller-Goymann, C. C. Drug release and permeation studies of nanosuspensions based on solidified reverse micellar solutions (SRMS). *Int. J. Pharm.* **2005**, *305*, 167–175.
- (29) Morrison, P. W. J.; Connon, C. J.; Khutoryanskiy, V. V. Cyclodextrin-Mediated Enhancement of Riboflavin Solubility and Corneal Permeability. *Mol. Pharmaceutics* **2013**, *10*, 756–762.
- (30) Qi, H. P.; Gao, X. C.; Zhang, L. Q.; Wei, S. Q.; Bi, S.; Yang, Z. C.; Cui, H. In vitro evaluation of enhancing effect of borneol on transcorneal permeation of compounds with different hydrophilicities and molecular sizes. *Eur. J. Pharmacol.* **2013**, *705*, 20–25.
- (31) Jingjing, L.; Shaoying, F.; Nan, W.; Yongsheng, H.; Xiaoning, Z.; Hao, C. The effects of combined menthol and borneol on fluconazole permeation through the cornea ex vivo. *Eur. J. Pharmacol.* **2012**, *688*, 1–5.
- (32) Diebold, Y.; Calonge, M. Applications of nanoparticles in ophthalmology. *Prog. Retinal Eye Res.* **2010**, *29*, 596–609.
- (33) Loftsson, T.; Masson, M. Cyclodextrins in topical drug formulations: theory and Practice. *Int. J. Pharm.* **2001**, *225*, 15–30.
- (34) Bary, A. R.; Tucker, I. G.; Davies, N. M. Considerations in the use of hydroxypropyl-b-cyclodextrin in the formulation of aqueous ophthalmic solutions of hydrocortisone. *Eur. J. Pharm. Biopharm.* **2000**, *50*, 237–244.
- (35) Hao, J.; Li, S. K.; Liu, C.-Y.; Kao, W. W. Y. Electrically assisted delivery of macromolecules into the corneal epithelium. *Exp. Eye Res.* **2009**, *89*, 934–941.
- (36) Kaur, H.; Ahuja, M.; Kumar, S.; Dilbaghi, N. Carboxymethyl tamarind kernel polysaccharide nanoparticles for ophthalmic drug delivery. *Int. J. Biol. Macromol.* **2012**, *50*, 833–839.
- (37) Sharma, R.; Ahuja, M.; Kaur, H. Thiolated pectin nanoparticles: Preparation, characterization and ex vivo corneal permeation study. *Carbohydr. Polym.* **2012**, *87*, 1606–1610.
- (38) (a) Muchtar, S.; Abdulrazik, M.; Frucht-Pery, J.; Benita, S. Ex-vivo permeation study of indomethacin from a submicron emulsion through albino rabbit cornea. *J. Controlled Release* **1997**, *44*, 55–64. (b) Amrite, A. C.; Edlhauser, H. F.; Singh, S. R.; Kompella, U. B. Effect of circulation on the disposition and ocular tissue distribution of 20 nm nanoparticles after periocular administration. *Mol. Vision* **2008**, *14*, 150–160.

- (39) Khutoryanskiy, V. V. Advances in Mucoadhesion and Mucoadhesive Polymers. *Macromol. Biosci.* **2011**, *11*, 748–764.
- (40) Prydal, J. I.; Kerr-Muir, M. G.; Dilly, P. N. Comparison of tear film thickness in three species determined by the glass fibre method and confocal microscopy. *Eye* **1993**, *7*, 472–475.
- (41) Bernkop-Schnurch, A. Thiomers: A new generation of mucoadhesive polymers. *Adv. Drug Delivery Rev.* **2005**, *57*, 1569–1582.
- (42) Deutel, B.; Greindl, M.; Thaurer, M.; Bernkop-Schnürch, A. Novel Insulin Thiomer Nanoparticles: In Vivo Evaluation of an Oral Drug Delivery System. *Biomacromolecules* **2008**, *9*, 278–285.
- (43) Wollensak, G.; Spoerl, E.; Seiler, T. Riboflavin/Ultraviolet-A-induced Collagen Crosslinking for the Treatment of Keratoconus. *Am. J. Ophthalmol.* **2003**, *135*, 620–627.
- (44) Newsome, D. A.; Gross, J.; Hassell, J. R. Human corneal stroma contains three distinct collagens. *Invest. Ophthalmol. Visual Sci.* **1982**, *22*, 376–381.
- (45) Meek, K. M.; Fullwood, N. J. Corneal and scleral collagens—a microscopist's perspective. *Micron* **2001**, *32*, 261–272.
- (46) Meek, K. M.; Boote, C. The organization of collagen in the corneal stroma. *Exp. Eye Res.* **2004**, *78*, 503–512.
- (47) Saika, S.; Ooshima, A.; Shima, K.; Tanaka, S.; Ohnishi, Y. Collagen types in healing alkali-burned corneal stroma in rabbits. *Jpn. J. Ophthalmol.* **1996**, *40*, 303–309.
- (48) Lai, S. K.; Wang, Y.-Y.; Hanes, J. Mucus-penetrating nanoparticles for drug and gene delivery to mucosal tissues. *Adv. Drug Delivery Rev.* **2009**, *61*, 58–171.
- (49) Xu, Q.; Boylan, N. J.; Cai, S.; Miao, B.; Patel, H.; Hanes, J. Scalable method to produce biodegradable nanoparticles that rapidly penetrate human mucus. *J. Controlled Release* **2013**, *170*, 279–286.
- (50) Suh, J.; Choy, K.-L.; Lai, S. K.; Suk, J. S.; Tang, B. C.; Prabhu, S.; Hanes, J. PEGylation of nanoparticles improves their cytoplasmic transport. *Int. J. Nanomed.* **2007**, *2*, 735–741.
- (51) Xu, Q.; Boylan, N. J.; Suk, J. S.; Wang, Y.-Y.; Nance, E. A.; Yang, J.-C.; McDonnell, P. J.; Cone, R. A.; Duh, E. J.; Hanes, J. Nanoparticle diffusion in, and microrheology of, the bovine vitreous ex vivo. *J. Controlled Release* **2013**, *167*, 76–84.